Interactions of Cosmic-Ray Muons in a Thick Pb Absorber*†

S. H. NEDDERMEYER AND S. B. CURTIS‡
Department of Physics, University of Washington, Seattle, Washington
(Received 11 March 1963)

The experiment is a cloud-chamber study of the momentum losses of the sea-level cosmic-ray particles, in the range 1–20 GeV/c, in a 317-g/cm^2 Pb target, by measurement of curvature in an 11 000-G magnetic field before and after traversal of the target. The incident particles are filtered by 28-in. Pb, corresponding to a normal momentum loss of about 1 GeV/c. One set of data is taken with simple coincidences to give essentially a random sample of the incident particles, and a second set with a 3–4-fold coincidence requiring large pulses, equivalent to ~10 minimum ionization particles, in one or both of two proportional counters located below and in the middle of the absorber. The experiment is not highly precise; nevertheless, the first part, which is presumed to be dominated by the normal "probable" collision energy loss, gives a reasonably good test of the error analysis, and the second part shows larger fluctuations which are shown to be at least in qualitative agreement with normal electromagnetic processes of muons. The energy distribution of showers observed in the lower chamber in the second sample is also in qualitative agreement with expectations for muons. The positive excess of the selected particles, defined by $\eta=(N_+-N_-)/(N_++N_-)$, is 0.10 ± 0.04 for the entire experiment (exclusive of the visible shower events) compared with 0.11 ± 0.02, an average for several other workers. The primaries of the shower events, however, give $\eta=0.49\pm0.12$. It is shown that this result cannot reasonably be attributed to contamination by protons, and its is equally difficult to attribute the effect to errors.

I. INTRODUCTION

THE study of the interactions of high-energy particles by the direct measurement of momentum losses is an old kind of experiment which actually had considerable consequences in early cosmic-ray studies. Such observations helped to elucidate the qualitative features of the ordinary ionization and electron collision energy loss processes as well as identifying and measuring the large radiative losses of high-energy electrons in materials of high atomic number. The general absence of the radiative losses was an essential link in the proof that the sea-level particles were predominantly of a new kind,[1] later called muons. We refer to the discussion in the introduction of a previous paper[2] which is partly relevant to the present experiment. The further pursuit of momentum loss measurements by Wilson[3] in copper, lead, and gold showed that up to roughly 0.7 GeV/c the measurements were consistent with the theoretically expected electromagnetic collision loss, but that from there up to 2 GeV there was an indication of an excess loss for which no interpretation was given; a positive excess of the particles with high losses was attributed to protons. Ehrenfest[4] measured the losses in 9-cm Au for particle momenta up to 5 GeV/c with much thicker filtering above the apparatus and found no significant evidence for anomalous losses. The extension of such experiments, with improved accuracy, and to higher momenta is beset with obvious and well-known difficulties (as will also be evident from this paper). Nevertheless, some further progress can be made, and the argument for attempting it is simply that it *may* be a powerful means for detecting new particles and processes that hitherto have escaped observation. The experiment is indirect because the exact character of the primary event is lost in a thick absorber; on the other hand, it is of a more fundamental nature than, for example, the correlation of range distribution underground with the measured sea-level momentum spectrum. Studies of the latter kind, as carried out by the Cornell group,[5] provide a very powerful test of the average behavior of the particles; nevertheless much of the detail is lost which may partly be recovered by experiments of the kind reported here even though the measurements are qualitative. Among other things the present experiment provides the first direct observation of momentum losses of muons which with reasonable certainty can be attributed to bremsstrahlung of the muon, a process which first appeared in a spectacular way in the early cloud-chamber experiments in the form of electromagnetic showers emerging from a lead plate with no ionizing particle entering, and frequently accompanied by a parallel high-energy penetrating particle. Evidently the photons arose from a radiative process higher on the path of the accompanying particle. No sharp interpretation was possible until after the identification of the muon and the analysis by Christy and Kusaka[6] of the experiment by Schein and Gill[7] on

* Work supported in part by the Office of Naval Research and the National Science Foundation.

† Partial reports of this work are given in Bull. Am. Phys. Soc. **6**, 350 (1961); **7**, 463 (1962). Tabulations of the data, examples of the photographs, and discussions of some points not covered in this paper are contained in S. B. Curtis, thesis, University of Washington, 1962 (unpublished).

‡ Present address: Lockheed California Company, Burbank, California.

[1] S. H. Neddermeyer and C. D. Anderson, Phys. Rev. **51**, 884 (1937).

[2] R. F. Deery and S. H. Neddermeyer, Phys. Rev. **121**, 1803 (1961).

[3] J. G. Wilson, Proc. Roy. Soc. (London) **A166**, 482 (1938); **A172**, 517 (1939).

[4] P. Ehrenfest, Compt. Rend. **207**, 573 (1938).

[5] P. H. Barrett, L. M. Bollinger, G. Cocconi, Y. Eisenberg, and K. Greisen, Rev. Mod. Phys. **24**, 133 (1952); see also reference 13.

[6] R. F. Christy and S. Kusaka, Phys. Rev. **59**, 414 (1941).

[7] M. Schein and P. S. Gill, Rev. Mod. Phys. **11**, 267 (1939).

the ionization bursts under thick layers of lead, where it appeared that the bremsstrahlung of the muons was the dominant process.

The general idea of the present experiment is very simple, namely, to measure the momentum losses of particles (mostly muons) in traversing about 1 ft of material, in this case, lead, and try to correlate the observations with what one would expect on the basis of the known processes. The available apparatus and the (approximately known) errors are such that the measurements can be carried to considerably higher momenta than has been done heretofore. It was also expected that there should be large fractional losses by bremsstrahlung once in 1000 ft or so of lead, and some of these should stand out above the error distribution, or in some cases result in an electromagnetic shower emerging below the absorber. The results are in general accord with expectations in that (a) they extend to higher momenta the determination of the probable "collision" loss, (b) are in essential agreement with calculated error distributions based on measurements of no-field tracks, except for some systematic differences that are not understood, (c) show occasional large losses in rough qualitative agreement with the normal processes of muons, and (d) the energy distribution of showers below the absorber is consistent with results of a calculation from shower theory and the "known" cross sections for the various high energy electromagnetic events of muons. There are, however, some interesting discrepancies of an unexpected character which are treated in the discussion and will require further work to resolve.

II. THE EXPERIMENT

The main features of the collision loss processes, that is, those which ordinarily dominate the stopping of heavy particles, except for nuclear interactions, are by now so well known that it is convenient to regard them partly as a calibration device for testing the validity of the measurements and the error distributions. Further, the large fractional losses are so improbable that to observe them effectively it is essential to use some selection scheme depending on the presence of a detectable event, with the attendant uncertainty in the selection efficiency. The experiment is, therefore, done in two parts, one representing a random sample of the total flux selected by simple coincidences, and the second using a strongly biased sample in which large pulses are required in one or both of two proportional counters buried in the absorber. The first sample is expected to give a rough measure of the 'probable' loss; even large fluctuations in the observed individual losses must presumably be attributed mainly to errors. The second sample, representing in this experiment about a 2% selection (and a much longer operating time), is expected to show a meaningfully larger average loss and larger

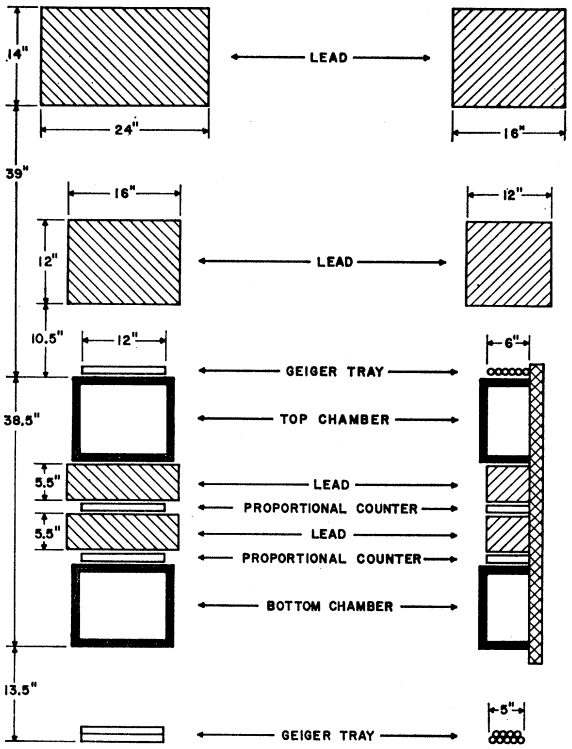

FIG. 1. Experimental arrangement.

fluctuations lying outside the error distribution. Electromagnetic events are generally distinguishable from nuclear, and among the former, those arising from bremsstrahlung (or perhaps other processes) may be distinguishable from the hard collisions with electrons if the fractional loss is large enough so that the conservation laws exclude the electron collision process. Otherwise, it is impossible in such a thick absorber to identify the various electromagnetic processes in individual events.

The experimental arrangement is shown in Fig. 1. The cloud chamber, 36 in. high, built in three sections, is the same one used in the earlier experiment,[2] but with the middle section removed and replaced by the lead absorber 28 cm thick, 317 g/cm². Two 15-cm×30-cm×2.5-cm proportional counters are placed, one in the middle and one below the absorber. Two GM trays are also placed as shown, and additional lead absorbers above. The first sample of data was taken with fourfold coincidences with low bias settings to require only a single minimum ionization particle (I_0) to traverse the four detectors. In the second sample the two proportional counters were biased to the equivalent of about 10 I_0 and 3–4-fold coincidences were required for which either one or both of the proportional counters delivered large pulses, and one or more counters in each GM tray fired. No restriction to one counter only in each tray was imposed for the latter, but the measurements reported here include only unaccompanied particles entering the absorber; this helps to bias in favor of the

selection of muons. The question of contamination by other particles is discussed in Sec. IV.

The aims of this preliminary experiment are necessarily of a somewhat qualitative, empirical, exploratory character, and the results give no really sharp test of any theory. We present enough of the results of the theory of the em processes for muons, as applied to this experiment, to give a qualitative idea of how the observations would be affected by the large losses. We also give an analysis of the effects of curvature errors superimposed on the probable collision loss regarded as a uniform (nonfluctuating) function of incident momentum. This treatment is essentially rigorous within the reasonable assumptions on which it is based. Finally, the showers observed in the lower chamber are discussed in terms of an application of shower theory to a calculation of the distribution of total energy appearing in charged particles.

The operating conditions of the apparatus are similar to those of the previous experiment. Similar procedures were used for track measurement, with primary reliance on the previously described curvometer. Since the tracks deviate in angle from the plane of the chamber face by about 5° or less, no correction was necessary for motion along the field. Approximate corrections were applied for variation of magnification and magnetic field with depth in the chamber by using the previously described calibration against the curvatures of current-carrying wires suspended in the field. These corrections are usually rather small, and even without them the most serious limitations for this experiment lie in the tracks themselves. The cloud chamber temperatures were monitored and the side to side differentials were typically about 0.02°C, occasionally below 0.01° or, unfortunately, as high as 0.05°. When thermal conditions were worse than this either definite distortions or else an increase in the spread of the measurements on an individual track could be observed. Some runs were discarded because of bad thermal conditions, as when the system went out of control.

III. THEORETICAL CALCULATIONS

In this section we give some of the necessary results of theory in graphical form without writing down the formulas, defining only such parameters as are necessary to make the discussion intelligible. All the essential theory is given in Rossi's book.[8] Our treatment of the errors, however, is probably new, and is given in more detail.

Ionization and Collisions with Electrons; Probable Energy Loss

The dominant energy loss process for muons, at least up to the region of hundreds of GeV is that of ionization in atomic collisions. It may conveniently be thought of in terms of two parts: (a) An interaction with the atom as a whole which results in very frequent transfers of energy that, in general, are not very large compared to the ionization energy, and (b) a direct interaction with individual electrons in which the conservation laws are satisfied between the two particles subject only to the limitations imposed by initial orbital momentum and the energy required to ionize. The two processes are evidently somewhat analogous to the photoelectric and Compton effects. Process (b) results in transfers, with decreasing probability, clear up to the maximum allowed, which may (at high incident energy) be a large fraction of the energy of the incident particle. For the purposes of this experiment it is useful to separate from the total collision loss that portion arising from individual energy transfers, w, less than some value, ξ, so chosen that the average number of transfers, per traversal of the absorber, with $w>\xi$ is one. The average energy loss so defined is a good approximation to the most probable collision loss and is sometimes called the 'probable' loss. Fluctuations below this level tend to be rather small and would be essentially unobservable in this experiment; however, fluctuations giving energy losses considerably larger than the probable are definitely expected to be observable. At the higher energies studied the probable loss itself is relatively so small as to be lost completely in the errors, but the larger, more improbable losses still are expected to have an observable effect.

For the thick absorber used in this experiment the value of ξ turns out to be fairly large. Thus, using the first term of the Bhabha formula (the classical Thomson-Bohr cross section) and ignoring the effect of the kinematic limit, w_m, we have

$$Ct\int_{\xi}\frac{dw}{w^2}=1, \quad \text{or} \quad \xi=Ct,$$

where

$$C=2\pi r_0^2 m_e c^2 NZ/A,$$

N is Avogadro's number, $r_0=e^2/m_e c^2$, and t=absorber thickness in g/cm^2=317 g/cm^2 of Pb. This gives ξ=19.3 MeV when $\xi\ll w_m$; but if w_m is taken into account we obtain for muons with E=1 GeV (for example), w_m=84 MeV, and ξ=11.5 MeV; or with E=2 GeV, w_m=310 MeV, and ξ=16 MeV. The biased sample of data may show the effects of such losses ($\gtrsim\xi$) occurring multiply in some cases (the Landau[9] fluctuations) for particles in the 1–2-GeV region.

The computed mean energy loss (including all collision losses up to w_m) as a function of initial mo-

[8] B. Rossi, *High Energy Particles*, (Prentice-Hall, Inc., Englewood Cliffs, New Jersey, 1952).

[9] L. D. Landau, J. Phys. U.S.S.R. 8, 201 (1944). A detailed investigation of the Landau fluctuations was not intended for this experiment. They should not be particularly enhanced in the high-pulse sample, because of the poor efficiency of the counters for detecting low-energy events. A much longer unbiased run would be required with more precise measurements and analysis than achieved in this experiment.

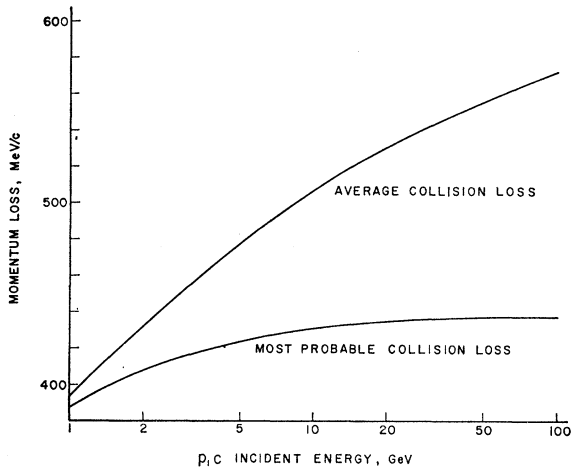

FIG. 2. Calculated average, and most probable, collision loss in 317 g/cm² Pb, including the polarization effect as treated by Sternheimer.

mentum is shown in Fig. 2 together with the probable value, both curves including the polarization effect as treated by Sternheimer.[10] Since the results are later given in terms of fractional momentum loss, the probable loss is shown again in that form in Fig. 3, together with curves for the Landau 5 and 10% limits (calculated from Symon's treatment[11]), representing the loss that is exceeded with 5 (or 10) % probability.[12]

Hard Collisions with Electrons; Bremsstrahlung and Direct Pair Production

The larger more improbable losses are the only ones that are expected to make an observable contribution

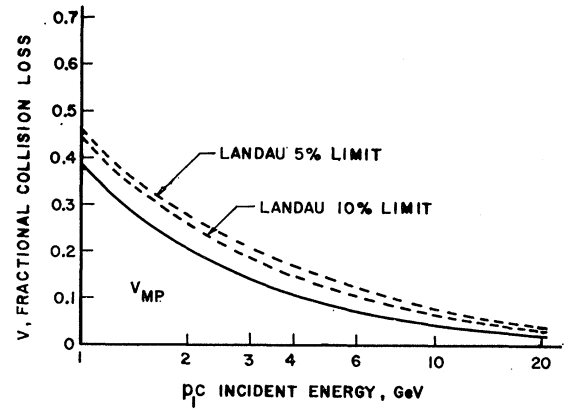

FIG. 3. Calculated probable collision loss in 317 g/cm² Pb. On the scale shown, the average loss is only slightly higher and is not given.

[10] R. M. Sternheimer, Phys. Rev. **88**, 851 (1952).
[11] K. R. Symon, thesis, Harvard University, 1948 (unpublished).
[12] On the scale of Fig. 3 the average loss is only slightly greater than the probable (see Fig. 2), and in this experiment we can hardly distinguish between them. The only reason for all this discussion is to provide a perspective for the principal subject under investigation, which is the very improbable large fractional losses.

to the fluctuations at higher energies. The calculated probability distributions for the various known processes for several muon energies are represented in Fig. 4 as probability per g cm^{-2} and per logarithmic interval of v, the fractional energy loss w/E, where w is the energy of the photon, electron (kinetic) or pair (total) involved in the process, and E is the initial (total, say) muon energy. The momenta in energy units are almost indistinguishable from the total energies, even for muons with momenta as low as 1 GeV/c. As we use later a probability function $P(E,v)$ defined as Prob$(w/E>v)$ (by a specified process per g cm^{-2} or per target traversal, according to context), the ordinate

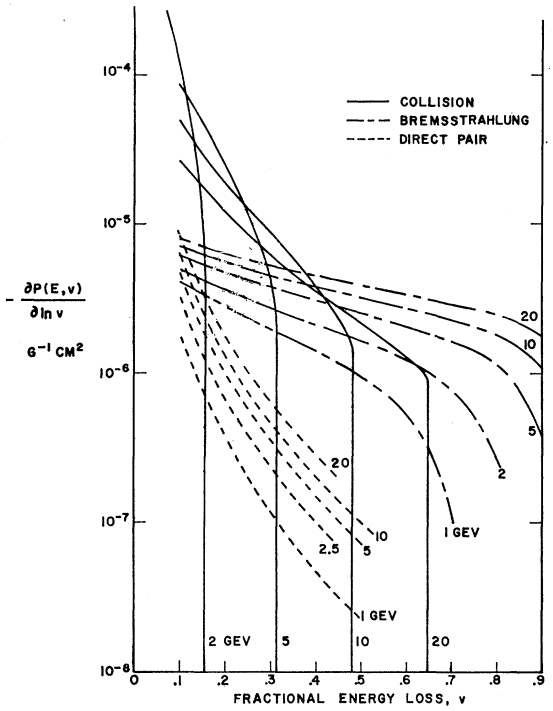

FIG. 4. Calculated differential probabilities for fractional energy losses per logarithmic interval of v and per g/cm² of Pb for the various electromagnetic processes and for various muon energies.

of Fig. 4 is specified in terms of P as $-dP/d\ \ln v$; thus

$$\int_v^{v_m} -dP = -P(E,v_m)+P(E,v) = P(E,v).$$

It is seen that the electron collisions dominate for small fractional losses, the radiation for large ones, and although the direct pair process competes with radiation at small v, its contribution, on the whole, is rather small and for the purposes of this experiment will not be discussed further. We have ignored entirely (except in the discussion of the results) all processes involving pion production or nuclear disintegrations produced by muons.

In Fig. 5 the curves of Fig. 4 for radiation and

collisions have been integrated over v and multiplied by the target thickness to obtain the integral distributions $P(E,v)=\text{Prob}(>v)$ per traversal; these have then been multiplied by the differential spectrum of the incident particles and the (solid angle×time) factor and plotted as functions of E, without including any efficiency factors. Thus,

$$dN=\Omega A\tau E(dj/dE)P(E,v)d\ln E,$$

where $\Omega A=10$ sr cm², $\tau=1.5\times10^6$ sec is the effective running time of the high-pulse part of the experiment, $dj/dE=$No. of muons per (cm² sec sr GeV) traversing the apparatus. The factor E is included to give the

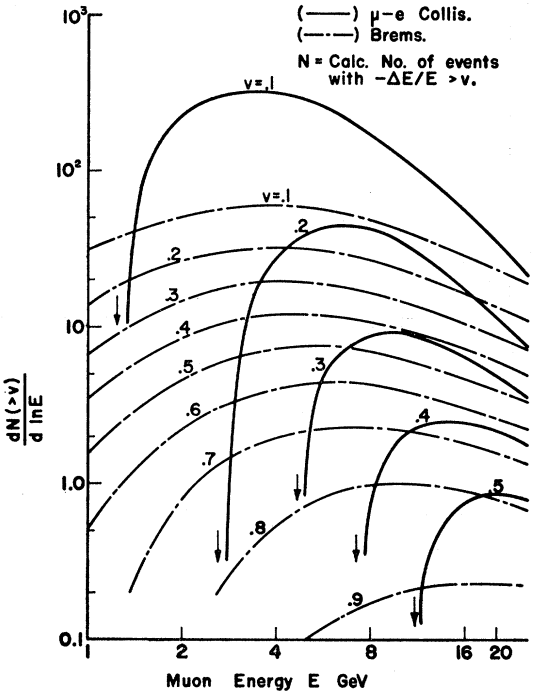

FIG. 5. Maximum numbers of events expected per logarithmic interval of muon energy with fractional losses greater than various values. Numbers correspond to entire high-pulse run (420-h. effective sensitive time) with no allowance for selection efficiency.

logarithmic scale of energy. Pine, Davisson, and Greisen's[13] spectrum was used for dj/dE with allowance made for 1-GeV loss of energy in the shield. It should be noted that the curves represent expected number of events of the particular type per dE/E for the entire effective time of the high-pulse experiment if events of all types and energies have detection probability of unity. In fact, the measurements presented include one-fourth the total (except for the showers). The efficiency of detection is discussed in a section below.

The numbers are presented in still one more way in Fig. 6, which shows the results of integrating over the

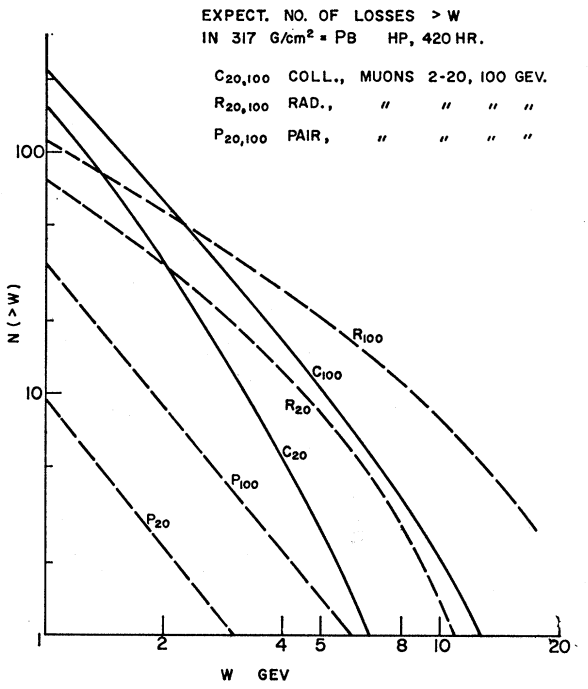

FIG. 6. Expected numbers of losses $>w$ by collisions, radiation and pair production for muons in 2–20 GeV and in 2–100 GeV. Numbers correspond to entire high-pulse run, efficiency ignored.

spectrum for various fixed values of the absolute energy loss, w. Thus, $\text{Prob}(-\Delta E>w)=P(E,w/E)$ and the total number of events anywhere in the target, with $-\Delta E>w$, produced by muons in $E_1<E<E_2$ is

$$N_{>w}=\Omega A\tau\int_{E_1}^{E_2}(dj/dE)P(E,w/E)dE. \qquad (1)$$

These numbers correspond (as does Fig. 5) to the total 420-h effective running time for the high-pulse experiment. They also represent the "source functions" used for the shower calculations below.

Showers

All the electromagnetic showers resulting from events in the target are expected to be almost completely absorbed except for the highest energy ones and those occurring in the bottom quarter or so of the target. The latter will appear in the lower chamber, and their measured energy distribution can provide another test of the behavior of the primary particles which is independent of the momentum-loss measurements. For the calculations we have used the results of the diffusion theory as developed by Bhabha and Chakrabarty[14] and calculated and tabulated by Jánossy and Messel.[15] Only the approximation 'A' (without ionization loss) was

[13] J. Pine, R. Davisson, and K. Greisen, Nuovo Cimento **14**, 1181 (1959).

[14] H. J. Bhabha and S. K. Chakrabarty, Phys. Rev. **74**, 1352 (1948).

[15] L. Jánossy and H. Messel, Proc. Roy. Irish Acad. **54**, 217 (1951).

used here and the analysis is applied only to that part of the shower energy contained in particles with individual energies ≥ 100 MeV.

Let $\Pi(w,E,t)$ stand for the appropriate shower function representing the average number of electrons (including positrons) of energy $>E$ emerging from the absorber in a shower initiated at height t by a photon (or electron or pair) of energy w, and $f(w)\,dw\,dt$ the number of initiating events of a particular kind in dw and dt. The latter is assumed independent of height (which it is, very nearly), and is related to the integral source functions (1) by $f(w)=(1/t_1)(-\partial N/\partial w)$, where t_1 is the total thickness in radiation lengths. Then if $g(W,w,t)\,dw\,dt$=No. of emerging showers with total electron energy $>W$ from events in $dw\,dt$ it follows that

$$g(W,w,t)=f(w) \tag{2}$$

since, in the approximation used, something always comes out, but generally strongly degraded in energy. The energy, W, is given by the integral over the shower function:

$$W=\int_{E_{\min}}^{w}-(\partial\Pi/\partial E)E\,dE=-\int E\,d\Pi$$

$$=w\int_{E=E_{\min}}^{w}(-E/w)\,d\Pi. \tag{3}$$

The integral is conveniently evaluated graphically (Π is of the form $\Pi(w/E,t)$) and gives directly $W(w,t)$. The lower limit, $E_{\min}$, is chosen equal to the lowest electron energy included in the observations. Finally, the total number of showers with $W_{\text{obs}}>W$ is given by

$$G(W)=\int_0^{t_1}\int_{w(W,t)}^{w_{\max}}g(W,w,t)\,dw\,dt$$

$$=\frac{1}{t_1}\int_0^{t_1}N[w(W,t)]\,dt, \tag{4}$$

where N is just the integral source function of Eq. (1). The integral is evaluated by approximate numerical integration and the results are applied in Sec. IV.

Efficiency Factors

The precise interpretation of the data is hampered by only approximately known efficiency factors of two principal kinds: (i) the probability that a desired event will trigger one of the proportional counters, and (ii) the effect of scattering in the absorber and curvature in the magnetic field. To improve the first we should perhaps have about four proportional counters rather than only two, as even a fairly large shower can get nearly completely absorbed in a few inches of lead. However, it has been shown by Greisen[16] that a tail of low-energy photons penetrates considerably farther than the main body of the shower, and this seems to be an important effect in the present experiment. It is probable that a considerable fraction of the observed events are triggered by low-energy electrons, produced by the photon tail, that are curled up inside counters by the magnetic field. Both this effect and (ii) have been considered by Curtis[17] and only the results are given here in Figs. 7 and 8. They can be regarded only as rough approximations in their actual application to this experiment.

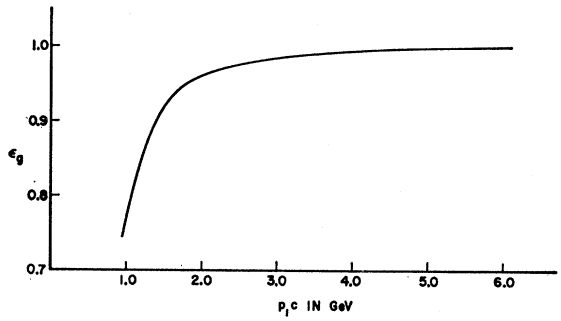

FIG. 7. Estimated geometrical efficiency.

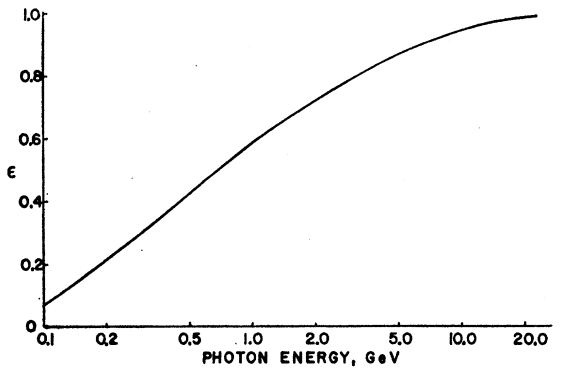

FIG. 8. Estimated photon detection efficiency under 160 g/cm² Pb.

Errors

In the following paragraphs we examine the effect that an idealized Gaussian error distribution in the measured curvatures has on the measured fractional momentum loss when the actual loss is assumed to be a nonfluctuating function of initial momentum equal to the calculated probable "collision" loss for the 317 g/cm²-Pb target used in this experiment. Let p_1, p_2 be the actual initial and final momenta, and $c_1=1/p_1$, $c_2=1/p_2$, the corresponding 'true' curvatures expressed as reciprocal momenta (or equivalent momenta in the case of zero-field measurements). The 'true' fractional momentum loss is then $v=(p_1-p_2)/p_1=1-c_1/c_2$. Let ξ_1, ξ_2 be the error variables for c_1, c_2; θ, that for v (that

[16] K. Greisen, Phys. Rev. **75**, 1063 (1948).

[17] S. B. Curtis, thesis, University of Washington, 1962 (unpublished).

is, $c_{1\text{meas}}=c_1+\xi_1$, etc.). Then

$$\theta=c_1/c_2-(c_1+\xi_1)/(c_2+\xi_2). \tag{5}$$

Assume that ξ_1, ξ_2 are independent and Gaussianly distributed with the same standard error, σ. From (5) it follows that $\theta=$const is a family of straight lines with the common point $(\xi_1,\xi_2)=(-c_1,-c_2)$; $\theta=0$ contains the origin as well. The probability distribution in θ is evidently given by a suitable integral over a portion of the ξ_1, ξ_2 plane bounded by θ, $\theta+d\theta$. To obtain a convenient form for the integral, define $r=+[(c_1+\xi_1)^2+(c_2+\xi_2)^2]^{1/2}$ and let $g(\xi_1)g(\xi_2)d\xi_1 d\xi_2$ be the Gaussian ξ distribution. The desired distribution $H(\theta)d\theta$, must be given by $H(\theta)d\theta=d\theta\int h(r,\theta)dr$, where

$$h(r,\theta)drd\theta=g[(\xi_1(r,\theta)]g[\xi_2(r,\theta)]J(\xi_1,\xi_2/r,\theta)drd\theta.$$

Evaluation of the Jacobian gives $J=r/(1+\eta^2)$ with $\eta=(c_1/c_2)-\theta$. The normal Gaussian for $\xi_{1,2}$ is

$$g(\xi)=[1/(2\pi)^{1/2}\sigma]\exp(-\xi^2/2\sigma^2)$$

and, expressing $\xi_1^2+\xi_2^2$ as a function of r and θ, $h(r,\theta)$ is found to be

$$h(r,\theta)=\frac{1}{2\pi\sigma^2}\cdot\frac{r}{1+\eta^2}\exp\left[-\frac{1}{2\sigma^2}(r^2\mp 2Br+C)\right]=h_{\mp},$$

with

$$B=(c_1\eta+c_2)/(1+\eta^2)^{1/2};\quad C=c_1^2+c_2^2.$$

In performing the integration over r some care has to be exercised because of the sign ambiguity of h. The final distribution is given by $H(\theta)=\int_{r=0}^{\infty}(h_-+h_+)\,dr$, the $(-)$ corresponding to the part of the distribution above $\xi_2=-c_2$ and the $(+)$ to that below. The situation should be clear from the diagram, Fig. 9, which illustrates a typical case with $c_2>c_1>0$. As θ goes from $-\infty$ to $+\infty$ the θ line sweeps the upper half-plane (above $-c_2$) once from right to left, and the lower from

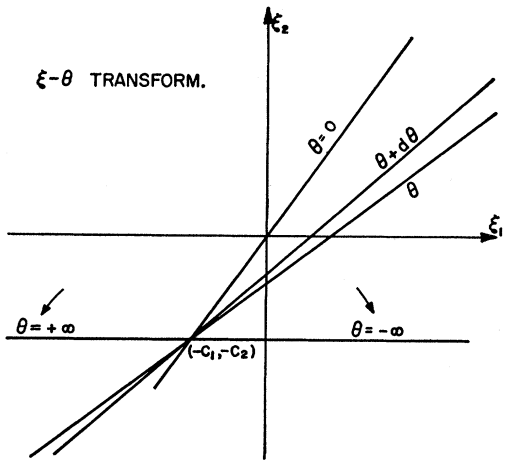

FIG. 9. Relation between the variable θ and the ξ_1, ξ_2 error space.

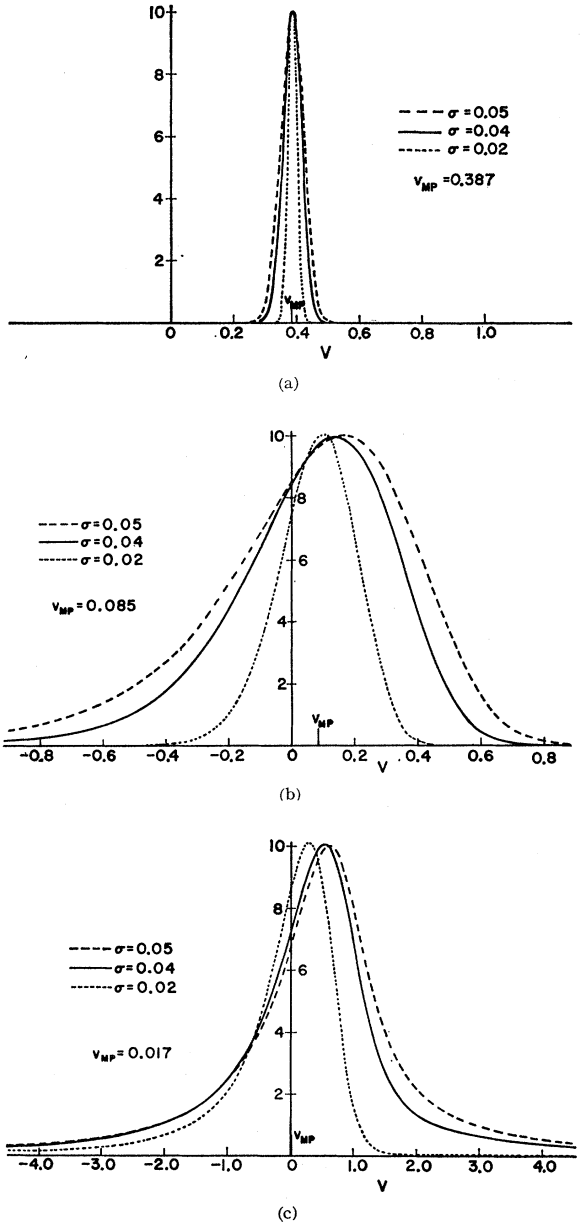

FIG. 10. The error function $H(\theta)$, arbitrarily normalized to same height, as it would affect v_{prob} assumed to be a definite non-fluctuating function of incident momentum; for (a) 1 GeV, (b) 5 GeV, and (c) 25 GeV. Here $\theta=v-v_{\text{prob}}$.

left to right. The result for $H(\theta)$ is

$$H(\theta)=\frac{e^{-C/2\sigma^2}}{\pi(1+\eta^2)}\left\{1+\frac{B}{\sigma}e^{B^2/2\sigma^2}\int_0^{B/\sigma}e^{-t^2/2}dt\right\}. \tag{6}$$

Since the original ξ distribution was normal, $H(\theta)$ also has to be normal. Plots of H, arbitrarily normalized to the same *height*, are shown in Fig. 10 for various initial momenta and various assumed values of σ. The value of $c_2=1/p_2$ is in each case determined by the probable

TABLE I. Summary of main parameters.

	Low pulse	High pulse (meas. sample)	High pulse (total)
ΩA (solid angle×area)	10.3	10.3	10.3 cm² sr.
Eff. oper. time	3.06	106	420 h
No. of events	291(1–20 GeV)	308(1–20 GeV)	51 (EM showers) 5 (nuclear)
Calc pri. flux {1–20 GeV	460	1.63×10^4	6.35×10^4
Calc pri. flux {2–100 GeV	...	...	4.75×10^4
Events/calc. flux	0.63	0.019	1.07×10^{-3}(EM showers) 1.05×10^{-4}(nuclear)

collision loss in the 317 g/cm²-Pb target for the corresponding initial momentum $p_1=1/c_1$. On the abscissa, θ represents the difference $v-v_{\text{prob}}$. One point to be noted especially is the way in which the most probable observed v is expected to shift more and more strongly to higher values as the errors become more dominant at the higher initial momentum. $H(\theta)$ includes all cases of spurious momentum losses or gains and sign reversal arising from the Gaussian error distributions in curvature.

Although the distribution $H(\theta)$ is presumably rigorous within the stated assumptions, it is not the appropriate one for direct comparison with the plots of the measured v's against the *measured* p_1's. The effect of measurement error in p_1 is taken into account as far as its effect on v is concerned, but $H(\theta)$ applies only to the case in which p_1 is precisely known. The necessary refinement is easy to formulate and probably not too hard to carry out approximately, but there are other refinements also of equal importance for a more complete analysis of the data, which we do not attempt in this paper. It will be seen below that the neglect may be partly responsible for certain peculiarities in the comparison with the data. The analysis is nevertheless useful as a qualitative guide.

IV. RESULTS

The principal integral quantities of the experiment are summarized in Table I. A scatter plot of the measurements of the fractional momentum loss

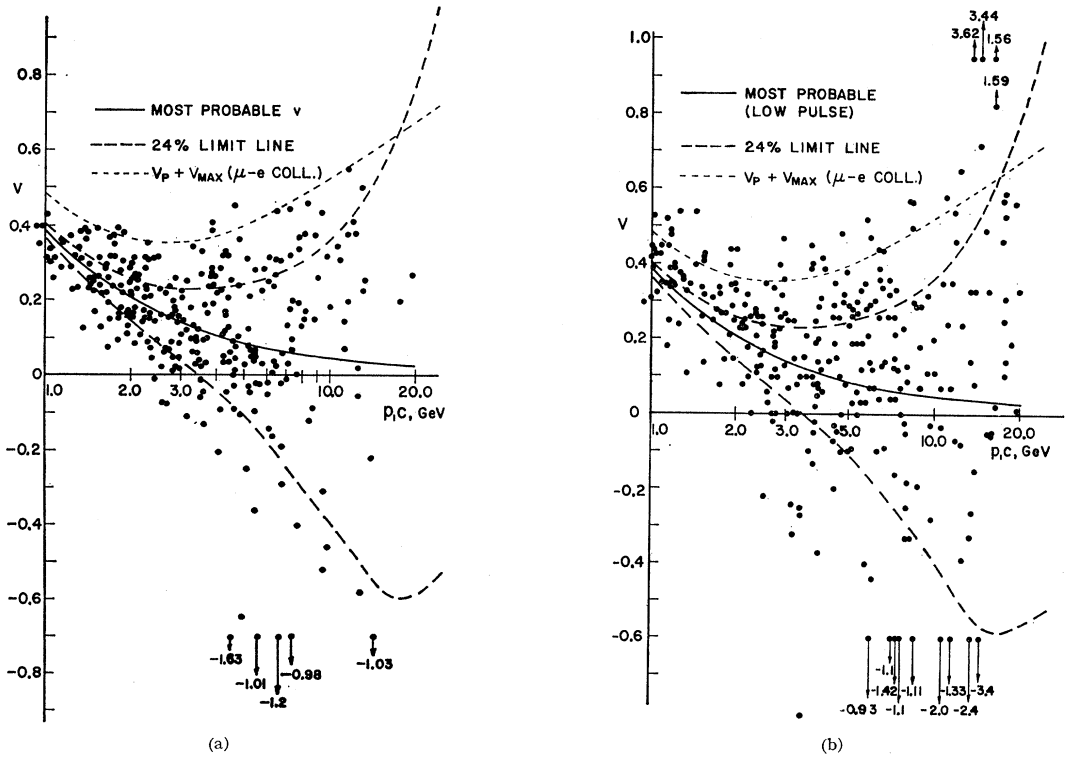

(a) (b)

FIG. 11. (a) Scatterplot of the momentum-loss measurements for the unbiased (low-pulse) data. The heavy dashed lines represent the limit lines such that errors should have thrown 24% of the points above the upper and 24% below the lower curves. The topmost curve represents the kinematic limit for μ-e collisions added to the probable loss. (b) Same for high-pulse sample. These represent one quarter of the entire high-pulse data, or 105-h effective sensitive time.

$v=-\Delta p/p_1$, versus initial momentum p_1, is shown in Fig. 11(a) for the low-pulse data and in 11(b) for the high pulse, compared in both cases with the same 'probable' collision loss as defined in Sec. III. Error bands are also shown, based on the curves of Fig. 10 for $\sigma=1/25$ GeV,[18] such that if the actual momentum loss were a definite nonfluctuating function of the momentum, and equal to the probable collision loss, then in the average errors should throw 24% of the points above and 24% below the band. The observed percentages (above; below) are (25±3; 20±3) for the low pulse and (35±3; 15±2) for the high pulse. The first pair of numbers (%) may be regarded as a rather good verification of the treatment of the errors, especially as, even in those measurements there may be expected a slight upward shift because of actual physical fluctuations. In the second case, the 11% difference (35%−24%) must be attributed principally to individual events involving appreciable fractional momentum losses. Independent measurements of smaller samples of the same data made without any corrections for variations in field and magnification gave nearly the same percentages, although in some individual cases there were rather bad discrepancies in momentum measurements which probably have to be attributed to a combination of human fatigue and variations in track quality.

To see in more detail how the measured v values compare to the error bands, we have plotted in Fig. 12 for the LP (low-pulse) and HP (high-pulse) data and for each of four momentum groups the fractional distribution of points in the upper (U) and lower (L) bands: $U(v>v_U)$; $L(v<v_L)$, where v_U, v_L represent the (upper, lower) 24% boundaries. From Fig. 12 the accentuation of the top band, U, and the depletion of the lower band L relative to the LP data are clearly evident, although there is for both a dissymmetry appearing as an average upward shift at low momenta and downward at high. The fact that the u, l points (lower case letters=low pulse) do not approximately coincide with the 24% line is probably in part connected with the faulty error analysis already mentioned in Sec. III; in fact, an improved analysis would tend to shift them in the right direction (up on the right and down on the left). Without attempting any correction of this discrepancy here, we, nevertheless, regard the difference between U and the average, $(u+l)/2$, as some measure of the real physical effect in the HP data. The difference amounts to 29% for the 1–2-GeV/c group and 11% (2–5), 8% (5–10), 7% (10–20), for the

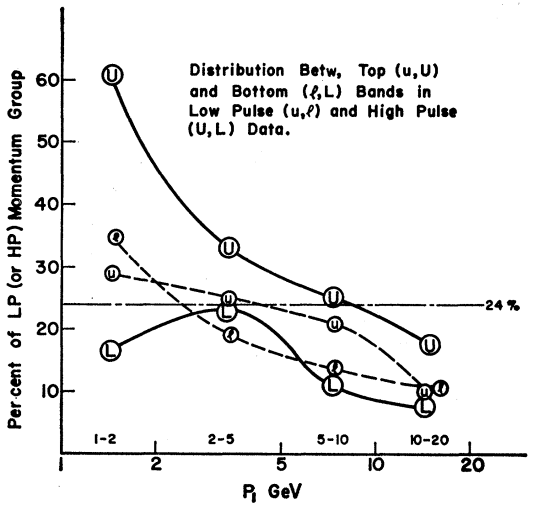

FIG. 12. Distribution between upper and lower error bands (above the upper and below the lower 24% lines) by momentum groups.

others. These correspond to 13% of the entire sample lying above the 24% line in addition to those expected to be there because of errors. (Compare with the 11% *supra*.)

A scatter plot of the shower data (which includes the entire HP sample) is shown in Fig. 13, with the same v_P(calc) curve and 24% limit lines shown for reference. The two large circles represent cases in which a single incident particle definitely produced a nuclear type event and in which a particle that might have been the primary emerged in the lower chamber. There were altogether only five "nuclear" events which otherwise satisfied the selection criteria. Excluding the two above

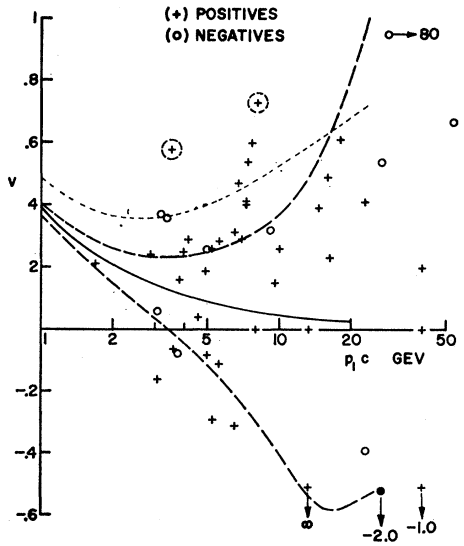

FIG. 13. Scatterplot of momentum-loss measurements in which an electromagnetic shower emerged in the lower chamber. These include the entire high-pulse run. Curves are the same as in Fig. 11.

[18] The use of $\sigma=1/25$ GeV in the analysis reflects a certain optimism that experimental conditions in the average would be better than they actually turned out to be. The mean for the no-field tests for this experiment gave 1/21 GeV compared to 1/22 for the μ-e experiment (Ref. 2). The over-all effective value for this experiment was likely between 1/21 and 1/25, and the current value may be somewhat better than 1/25. See Ref. 17 for a discussion of the identification of a heat leak and its correlation with track distortion.

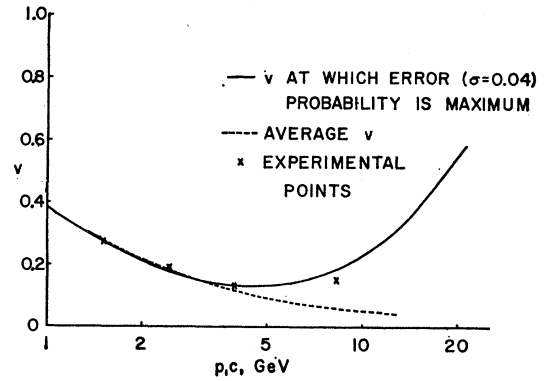

FIG. 14. Average momentum loss for a sample of 188 tracks in the low-pulse data. Lower curve is the calculated average v, slightly higher than v_p. Last point shows shift toward most probable *measurement* based on the error analysis.

cases, 41% of the points in the 1–20-GeV/c range lie above the upper 24% line, and 16% below the lower. Making a 5% correction based on the u, l curves of Fig. 12, we find then about $41-24+5=22\%$ of the points above the effective 24% line *in addition to* those expected to be there because of errors. Summary: 13% of the points on the HP plot and 22% of the points on the HP shower plot lie above the (effective) 24% reference line *in addition to* those expected to be there on account of errors.

The Low Momentum Region (1–2 GeV). The Landau Fluctuations

The picture presented in the preceding paragraphs is far from a satisfactory one, although it is clear both that the errors are producing fluctuations of the general character expected and that many of the large fluctuations shown in the HP sample must correspond to real physical effects. However, in the 1–2-GeV region there are, even in the LP sample, some apparent losses that are too large to understand either as errors or as normal physical effects. Here we expect a few events representing appreciable single losses above the probable and a few more representing multiple losses of the order of ξ, but these can hardly account for the observations. Further discussion of this part of the data is not particularly illuminating and we have to leave the question for later work.

Average Momentum Loss for the Low-Pulse Data

A plot of the average measured fractional loss for a sample of 188 tracks as a function of momentum is shown in Fig. 14, in comparison with the calculated v_{av} and the calculated most probable *measurement* of v_{av} based on the error curves of Fig. 10. It is seen that there is a definite tendency for the measured points to shift upward, somewhat as expected from the errors. This may be the explanation of the apparent "anomalous" losses obtained by Blackett and Wilson at the higher momenta.

The High-Pulse Data

We give here a further brief qualitative discussion which purports only to show that the observed fluctuations in the middle and higher momentum region may be qualitatively consistent with the normal behavior expected of muons. The scatter plot of Fig. 11(b) represents one quarter of the entire high bias run, including 13 of the shower events of Fig. 13 which it happened to contain.

In Table II we have listed $N_{\text{obs}}-N_{\text{err}}$, taken from Fig. 12 and expressed as percent of N, the number in the corresponding momentum interval; then v_U-v_P (column 4) is taken wholly arbitrarily as a basis for calculating the "expected" number of losses for approximate comparison with $N_{\text{obs}}-N_{\text{err}}$. The numbers in parentheses in column 4 represent arbitrary alternative values of v which could be equally valid guesses for such a crude analysis. The numbers listed under N_{calc} (last four columns) are obtained by use of the curves of Fig. 5 and the efficiency of Fig. 8. The final percentages (column 8) either approximately equal or bracket those of column 1 (except for 1–2 GeV, discussed above) and we feel justified in concluding, until better experiments and a more elaborate analysis can be made, that the experiment definitely shows the presence of large losses which are not inconsistent with normal expectations for muons. Summary: In the

TABLE II. Observed fluctuations, compared to very qualitative calculations. (See text.)

Momentum interval (GeV)	No. in interval N	$N_{\text{obs}}-N_{\text{err}}$[a] (percent of N)	v_U-v_P[b]	N_{calc} with $v>v_U-v_P$ Coll	Rad	Tot	Tot, % of N
1–2	61	29			(Partly multiple, see text)		
			(0.10)	(2.4)	(1.0)	(3.4)	(5.5)
2–5	110	11	0.10	24	4.2	28	25
			(0.20)	(1.7)	(3.4)	(5.1)	(4.6)
5–10	84	8	0.21	4.5	3.1	7.6	9
10–20	50	7	0.46	0.2	1.0	1.2	2.4
			(0.20)	(2.8)	(2.5)	(5.3)	(10.6)

[a] The number lying in the U band minus the number expected to be there because of errors.
[b] Average difference between v at the U boundary and the 'probable' v.

1–2-GeV/c interval the events contributing to the observed fluctuations are partly multiple, and partly single collision losses, but the apparent abnormal number of large fractional losses is not understood. In the 2–10-GeV interval the largest losses are mainly single, with radiation and collisions contributing about equally, and at 10–20 GeV the radiative events are slightly predominant. There is no significant discrepancy observed in the 2–20-GeV interval.

Showers

The shower data (scatter plot of $-\Delta p$, Fig. 13) represent all the cases in the entire high-pulse run in which the particle traversing the Pb was accompanied by a shower in the lower chamber containing one or more particles, besides the primary, with an aggregate energy exceeding 100 MeV. As shown above, the shower primaries have a considerably stronger bias toward large momentum losses, and as will be seen in the next section they have also a strong bias toward higher primary momenta. We do not attempt here any analysis like that of the preceding section, but instead only apply the shower theory as given in Sec. III. For this purpose we plot in Fig. 15 the observed integral distribution of shower energies, W, where W is the energy of a particular event appearing in the lower chamber in the form of charged particles with *individual* energies >100 MeV. The 100-MeV minimum electron energy should be sufficient to assure the validity of "Approximation A." The points (⊗) represent the results of the shower calculation described in Sec. III for collisions, radiation and direct pair production by muons in the range 2–100 GeV. The (×) represent the part contributed by $\mu-e$ collisions only. The symbols (⊙) and (●) represent for comparison the corresponding results for muons in the 2–20-GeV interval. The effective range of muon energy is not well defined, but 2–100 GeV is probably a good approximation. For that case the calculations give a better fit, although the absolute normalization is not to be trusted. For the showers, however, the detection efficiency of the proportional counter may properly be assumed to be unity, since the probability of the shower getting into the lower chamber has been taken into account. In the above calculations the direct pair contribution represents only a negligible fraction of the total (1 event with $W>0.5$ GeV and 0.3 with $W>1.0$).

Momentum Distributions of the Selected Incident Particles

Any biased selection scheme must produce a distortion of the selected momentum spectrum in comparison to the total incident one, which depends, among other things, on the variation of event probability with primary energy and of selection efficiency with event energy. In fact, the spectrum that should be selected can be calculated from the fundamental

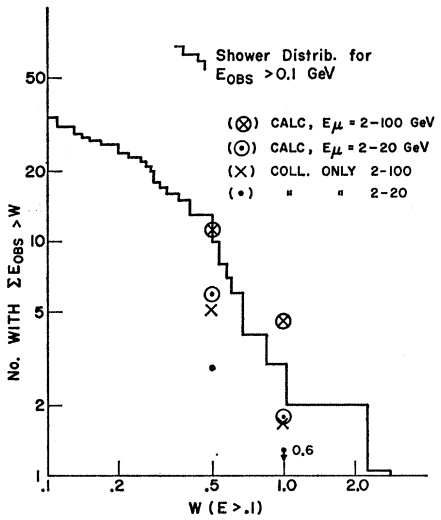

FIG. 15. Observed distribution of total shower energies contained in particles with individual energy >0.1 GeV (excluding primary particle).

cross sections and the properties of the system and, thus, provide a somewhat different kind of test for the behavior of the particles. We do not attempt any such analysis here and only exhibit the observed integral spectra of the incident particles for the three cases in Figs. 16, 17, and 18, with the integral Cornell spectrum[13] shown for comparison (corrected by 1 GeV to allow for absorption in the Pb shield). Except for the shower events (Fig. 18) the spectra were arbitrarily cut off at

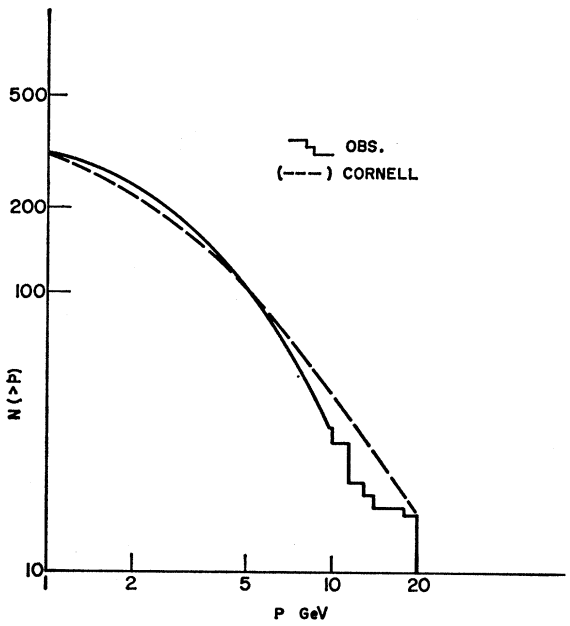

FIG. 16. Momentum distribution of particles selected by the low-pulse experiment, compared to the Cornell spectrum, which should be close to that for Seattle. This and the plots of Figs. 17 and 18 are given as unanalyzed measurements (see text).

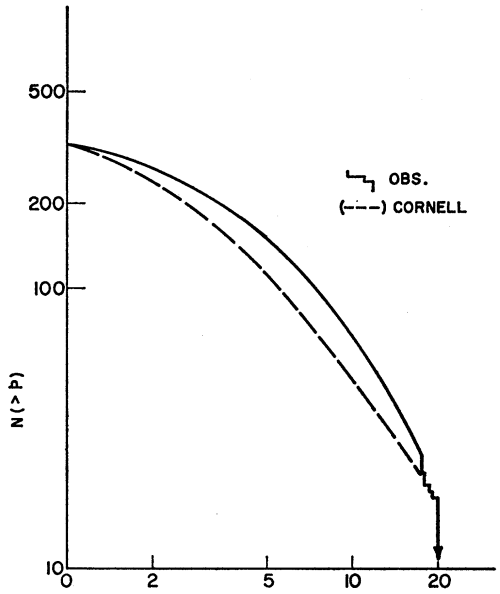

FIG. 17. Momentum distribution for high-pulse sample.

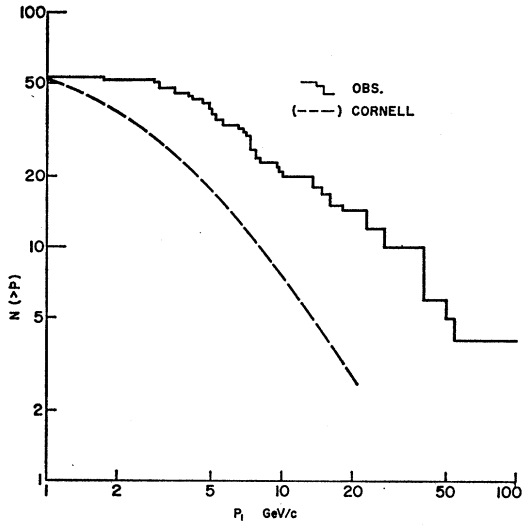

FIG. 18. Momentum distribution of shower primaries.

20 GeV/c for the measured value of the incident momentum, since little or no meaning could be attached to momentum loss measurements beyond there. No actual count was made of the number of particles above cutoff and the comparison is therefore made by the following normalization. Let $F(p)$ be the reference spectrum (No. with mom.$>p$) and N the total number of particles with measured momenta in (1–20 GeV). Put $N=K[F(1)-F(20)]$. This determines the normalization factor K. In the graphs of Figs. 16 and 17 the quantity $N_{\text{obs}}(>p)+KF(20)$ is compared with $KF(p)$. This simply fits the spectra at both ends of the range and allows a convenient representation of the relative distortion in the observed spectrum. Since there is no upper cutoff on the shower primaries, the only normalization made there (Fig. 18) is at $p_1=1$.

The general character of the observed spectra is about as expected, with a very noticeable shift to high momenta in Fig. 17 and a very much stronger shift in Fig. 18. The form of the latter distribution above 20 GeV is to a considerable degree determined by errors. (Here both chambers cannot be used to extend the range of reliable momentum estimates to the degree that was possible in the μ-e experiment). However, there can be no doubt that the effect is largely a physical one reflecting the simple fact that the high-energy events require high-energy particles to produce them. The depletion of particles near the 20-GeV limit in Fig. 16 can be seen to be in part due to errors, but further discussion of the spectra has to be left for a later study.

Positive Excess

The results for the positive excess of the incident particles selected by the various parts of this experiment are summarized in Table III. The observed values of the parameter $\eta=(N_+-N_-)/(N_++N_-)$ are listed for the LP and HP samples and for the HP shower producers (HPS), separated according to field direction. There is no significant difference between the first two, which give a combined average 0.10 ± 0.04 compared to the value 0.11 ± 0.02 representing an average of the results of several other workers for unbiased samples of the sea level particles. The change in η with field reversal probably has to be regarded as evidence for the presence of systematic track distortion, although the differences are not outside reasonable statistical fluctuations. The very large positive excess (0.49 ± 0.12) for the part of the high-pulse particles that produce observable showers is a wholly unexpected result which holds under field reversal and differs from the normal value by several standard deviations. It probably has to be taken seriously, although it appears difficult to understand in terms of known processes.

The interpretation that immediately suggests itself is that the large excess consists of protons. That this interpretation is untenable is to be seen in several ways. Let η_0 represent the normal positive excess (0.11) and η, that observed; then the required number of protons, N_p, to produce the observed η in the sample of 51 particles, is given by $N_p/(N_\mu+N_p)=(\eta-\eta_0)/(1-\eta_0)=0.43$, or $N_p=21$ protons. Now if protons comprise 1% of the incident particles,[19] then about 250 above 5 GeV are incident in the data sample containing the showers. If the *absorption* path, λ, is taken as 300 g/cm^2, then there are 750 g/cm$^2=2.5\lambda$ in the Pb shield and 320 g/cm$^2\simeq\lambda$ between chambers; thus about 8 protons

[19] L. I. Potapov and N. V. Shostakovitch, Dokl. Akad. Nauk S.S.S.R. **106**, 641 (1956) [translation, Soviet Phys.—Doklady **1**, 85 (1956)]. See also, W. Pak and K. Greisen, Phys. Rev. **125**, 1668 (1962). They obtain 1.6 ± 1.1 for the proton percentage. This would not affect our conclusion.

might be expected to survive the total path and perhaps also produce events that could trigger the counters. Altogether 21 might have been expected to survive the upper absorber, but, in general, be accompanied by products of nuclear interactions and be rejected by visual selection, if not by the absorber and counters below. In fact, 5 unaccompanied particles were observed which produced events obviously nuclear in character, and two of these (both +) showed tracks below which could possibly be identified as the original particle. (Their v values are shown in dashed circles in Fig. 13.) On the basis of the absorption path used above we would have expected $e^{-1}=0.37$ of the five incident particles to survive, or two, as observed (but the $\lambda=300$ g/cm^2 is somewhat arbitrary and not too well defined). The observations are, therefore, quite consistent with what may reasonably be assumed is qualitatively known about the proton component without interpreting any of the main shower-producing group as protons.

The general character of the observed shower events, as well as the comparison with the calculations from shower theory, above, are entirely consistent with the assumption that the events are predominantly electromagnetic and that they have their origins in the processes normally expected of muons according to existing theory.

V. CONCLUSIONS; DISCUSSION

The results, insofar that they are in accord with general expectations, have already been summarized at the end of I. Apart from some possible trouble with understanding the fluctuations in the 1–2-GeV region, the principal difficulty lies in the interpretation of the large positive excess for the primaries of the observed showers. That it is very hard to attribute this excess to protons has been shown above with fairly cogent arguments based on experimental data, and partly on fundamental theory, the general validity of which there is little reason to doubt, although it was part of the (idealized) aim of this experiment to test the theory by direct or indirect means.

Further detailed discussion of these questions has to be left to later papers with more data, more accurate measurements and more precise analysis. Two further points may be mentioned however in connection with testing the validity of the positive excess. Besides the independent check of the signs and momentum loss measurements of the HPS sample mentioned in Sec. IV we also made similar checks of partial samples of the other data, as well as measuring total magnetic deflections on all of HPS and parts of LP and HP. This was done by means of a fine meter-long wire stretched on a drafting machine mounted on the projection table. Tangent angles were read with the wire fitted visually to the middle of the track in the top chamber, then in the bottom one. The change, $\Delta\theta$, of the tangent angle, multiplied by a suitable average of measured momentum (the harmonic mean was used) gives a number whose sign is expected to correspond with the sign of the particle and whose magnitude is expected to be roughly a constant proportional to the magnetic field strength multiplied by the distance between tangent points, but with a large random part superimposed, which represents scattering in the Pb as well as errors. These distributions show some interesting features which are not yet understood and may correspond to some of the difficulties above; the immediate point, however, is that, except for the tail in the distribution of $p\Delta\theta$ that may be attributed to scattering, the sign determinations agree almost completely with those of the initial analysis. It is, therefore, even less likely that the sign anomaly can be attributed to large accidental systematic errors.

The second point is that also in the earlier experiment on the collisions with electrons in carbon[2] an abnormal positive excess was found, namely, 0.23 ± 0.06, about twice the usual value. In view of the results of the present experiment as well as a continuation of the muon-electron experiment to be reported later, it now appears that the previous result may represent a real physical effect. A preliminary report of some of the newer results has already been given[20] and a further discussion will be published elsewhere.

TABLE III. Positive excess of the selected incident particles. Table gives values of the parameter $\eta=(N_+-N_-)/(N_++N_-)$ for low pulse (LP), high pulse (HP), and shower primaries (HPS) for original and reversed magnetic field directions (OF, RF).

Data	Sample	N_+	N_-	N	$\eta\pm\frac{2}{N}\left(\frac{N_+N_-}{N}\right)^{1/2}$
LP	OF	103	92	195	0.06 ± 0.07
	RF	57	39	96	0.19 ± 0.10
	Total	160	131	291	0.10 ± 0.06
HP	OF	95	91	186	0.02 ± 0.07
	RF	75	47	122	0.23 ± 0.09
	Total	170	138	308	0.10 ± 0.06
HPS	OF	16	5	21	0.52 ± 0.19
	RF	22	8	30	0.47 ± 0.16
	Total	38	13	51	0.49 ± 0.12

[20] P. Kotzer and S. H. Neddermeyer, Bull. Am. Phys. Soc. **7**, 463, (1962).